Electric Power Systems Research 180 (2020) 106135

Contents lists available at ScienceDirect

Electric Power Systems Research

journal homepage: www.elsevier.com/locate/epsr

Modeling the impact of GIC neutral blocking devices on distance protection relay operations for transmission lines☆

Emilio C. Piesciorovsky*, Alfonso G. Tarditi

Power and Energy Systems Group, Electrical & Electronics Systems Research Division, Oak Ridge National Laboratory, One Bethel Valley Road, Oak Ridge, TN, 37830, USA

ARTICLE INFO

Keywords:
Distance protection relay
Geomagnetic induced currents
Neutral blocking device
Transmission line
Apparent impedance

ABSTRACT

Geomagnetic Induced Current (GIC) blocking devices typically include a capacitor on the neutral grounding path of wye-configured transformers. This type of GIC blocking device was designed as an effective countermeasure to prevent possible damages caused on the power grid by geomagnetic storms, and by the slow-varying component of a high-altitude electromagnetic pulse (HEMP). The insertion of a capacitor in the transformer neutral impedes the establishment of GICs in lines terminated with wye-connected transformer windings. With the presence of a capacitively grounded neutral, however, it becomes important to evaluate that no adverse effects are introduced in the general grid operations. In this context, this study investigates the impact of GIC neutral blocking devices on the functionality of distance protection relays for different values of transformer neutral blocking capacitors, and at different transmission line voltages. This study was conducted with a real-time simulation platform, and the simulations were performed by introducing a phase-to-ground fault at different line locations, and by measuring the apparent impedance at the protection relay location. The results indicated that, for typical values of capacitance considered for GIC neutral blocking devices, the distance protection relay model operates properly, without requiring a modification of the relay settings.

1. Introduction

Geomagnetic induced current(GIC) blocking devices prevent the adverse impact of quasi-dc currents on transmission line transformers that can be induced by geomagnetic disturbances [1,2]. These devices consist primarily of capacitors connected to the neutral of wye-connected transformers [3]. The impact of quasi-dc induced currents on transmission lines has been studied in relation to heat damage in transformer windings [1,4–6], and malfunctions in protection relay operations [7,8]. While GICs are characterized by short-duration peaks windings and structural parts overheating do not pose a serious concern [9], more persistent GICs can lead to serious thermal damages [3]. To mitigate the GICs in large-scale power systems, line switching methods based on algorithms were studied [10,11], and the proposed algorithms optimized the switching strategy to minimize the effect of GICs. The optimal placement of GIC neutral blocking devices (NBDs) was studied considering equipment thermal limits, and power system operation constraints were evaluated [12]. Also, the impact of GICs on voltage fluctuations along the power system were studied by inserting grounding small resistances in neutral points to restrain voltage fluctuations in the power grid [13].

On the other hand, unlike heat-related damage, even a short-duration magnetic saturation of the transformer core may, in principle, lead to abnormal levels of harmonics that are enough to impact the functionality of distance relay protections. This issue was analyzed in [7,8], and it was shown that no malfunction of distance relay operations occurred, for a 500 kV transmission line. In [14] it was also shown that distance relays operate normally in transmission lines with GIC NBDs inserted, if the neutral grounding capacitance is greater than 1000 μF.

However, no dynamic analysis of fault apparent impedances has been performed or published to date [7,8,14]. In this paper, a detailed dynamic analysis was performed based on the simulation and plot of the phase-to-ground fault apparent impedance detected by the distance relay model implemented, and for different line lengths, and voltage

☆ This manuscript has been authored by UT-Battelle, LLC, under contract DE-AC05-00OR22725 with the US Department of Energy (DOE). The US government retains and the publisher, by accepting the article for publication, acknowledges that the US government retains a nonexclusive, paid-up, irrevocable, worldwide license to publish or reproduce the published form of this manuscript, or allow others to do so, for US government purposes. DOE will provide public access to these results of federally sponsored research in accordance with the DOE Public Access Plan (http://energy.gov/downloads/doe-public-access-plan).

* Corresponding author.
E-mail address: piesciorovec@ornl.gov (E.C. Piesciorovsky).

https://doi.org/10.1016/j.epsr.2019.106135
Received 19 February 2019; Received in revised form 8 October 2019; Accepted 28 November 2019
Available online 09 December 2019
0378-7796/

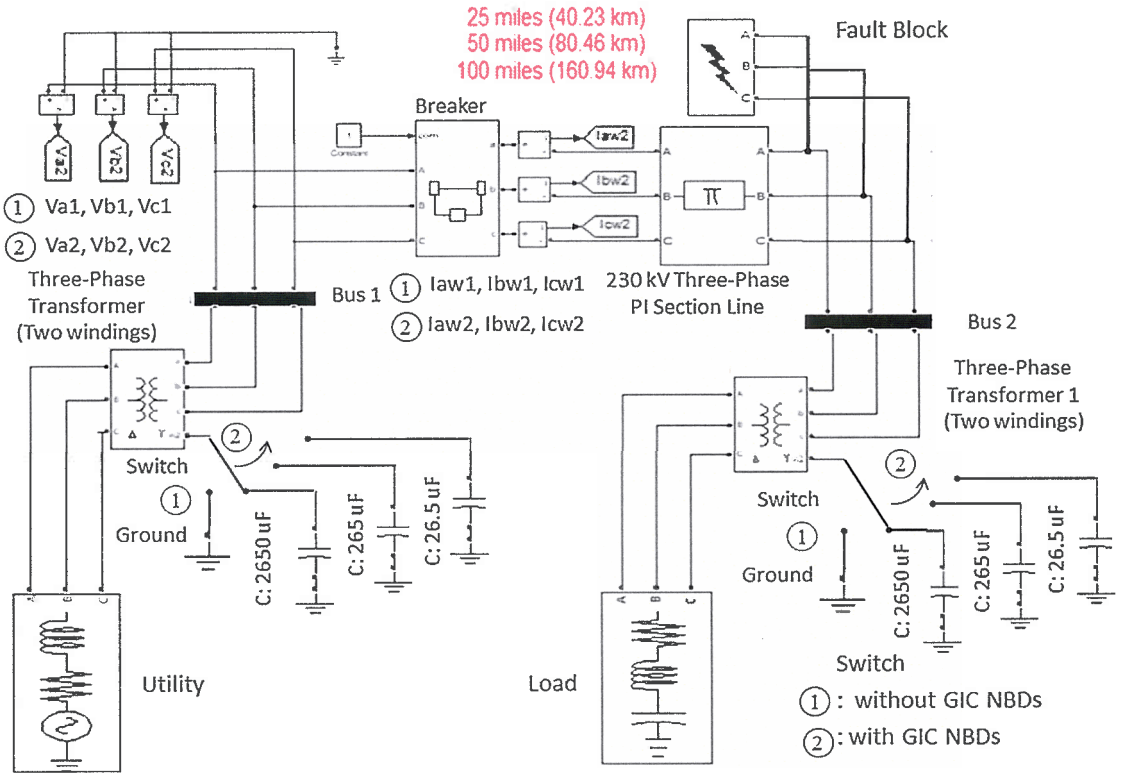

Fig. 1. Transmission line without (1) and with (2) GIC NBDs.

Table 1
Positive and zero-sequence impedances for the transmission lines [17,18].

Phase to phase voltage [kV]	Line length [km]	Positive and zero-sequence impedances of transmission lines per unit length				
		rl_1 (rl_0) [Ω/km]	xl_1 (xl_0) [Ω/km]	l_1 (l_0) [H/km]	b_1 (b_0) [μS/km]	c_1 (c_0) [F/ km]
230	40.23	0.06095862	0.47715862	0.00126570	3.462	9.18398×10^{-9}
	80.46	(0.2307241)	(1.57280689)	(0.00417200)	(1.906)	(5.05560×10^{-9})
	160.94					
345	40.23	0.03295172	0.48451821	0.00128522	3.469	9.20259×10^{-9}
	80.46	(0.31560913)	(1.18080586)	(0.00313218)	(2.529)	(6.70916×10^{-9})
	160.94					

rl_1, xl_1, c_1: positive sequence series resistance, reactance and capacitance per unit length (p.u.l.), respectively.
rl_0, xl_0, c_0: zero sequence series resistance, reactance and capacitance per unit length (p.u.l.), respectively.

Table 2
Zero-sequence current compensation factors K_0 for different cases of transmission lines.

Setting #	Line length		Phase to Phase Voltage [kV]	Zero-sequence current compensation factors	
	[km]	[miles]		Magnitude	Angle [Degrees]
1	40.23	25	230	0.768	−1.536
2	80.46	50			−1.521
3	160.94	100			−1.527
4	40.23	25	345	0.516	−18.183
5	80.46	50			−18.211
6	160.94	100			−18.208

levels, leading to variations in line source impedance ratios (SIR).

The distance sensing function of protection relays (mho relays) is commonly set by referring to a R–X diagram. This diagram represents the variation over time of the impedance of the transmission line [15] at the relay location (apparent impedance). The protection intervenes when the measured apparent impedance falls within an established circle in the R–X plane (e.g. as a result of a fault) [16]. In this study, the path of apparent impedances in the R–X plane during a phase-to-ground fault was compared with and without GIC NBDs inserted, and for different capacitance and SIR values.

2. The test scenario

The power system scenario was simulated with a real-time simulator. Distance protection operations for 230 and 345 kV transmission lines in a radial power system with a length of 25, 50 and 100 miles were considered. The 230 and 345 kV impedance parameters were collected from real transmission lines [17,18]. Three different capacitance values for the GIC NBDs were tested: 2650 μF (corresponding to 1-ohm reactance at 60 Hz), 265 μF, and 26.5 μF. The last value was purposely chosen as an extreme case, but it is too small for practical applications. A case without GIC NBDs provided the reference for the value of fault apparent impedances seen by the distance protection

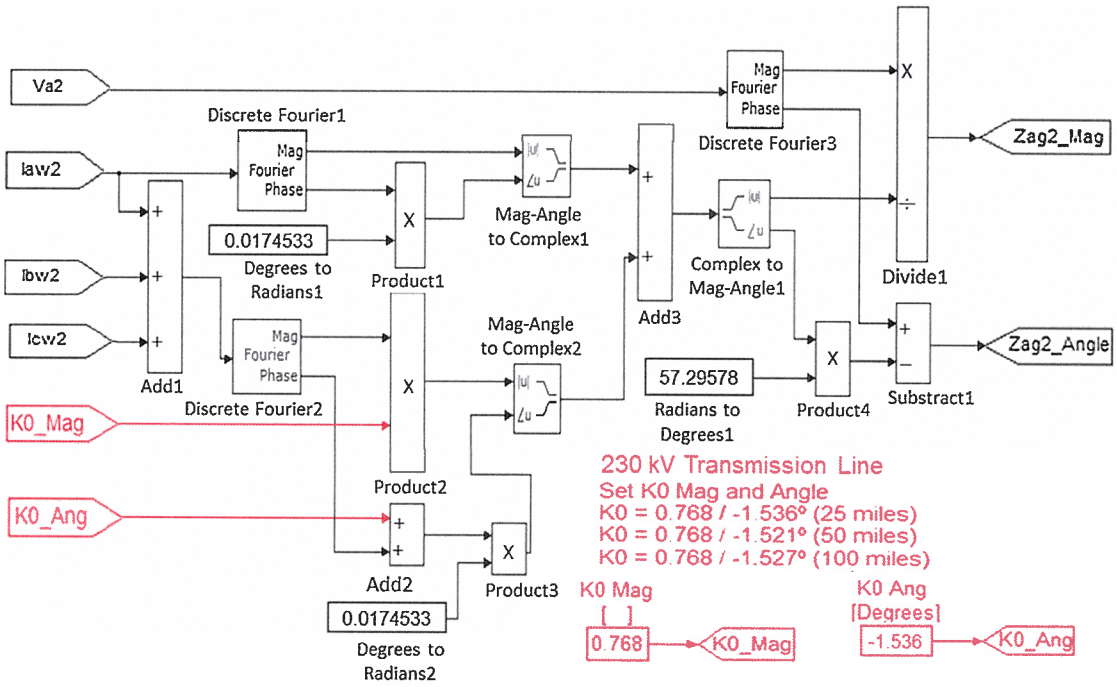

Fig. 2. RT-LAB Block to compute the phase-to-ground fault apparent impedance (e.g. for the 230 kV transmission line).

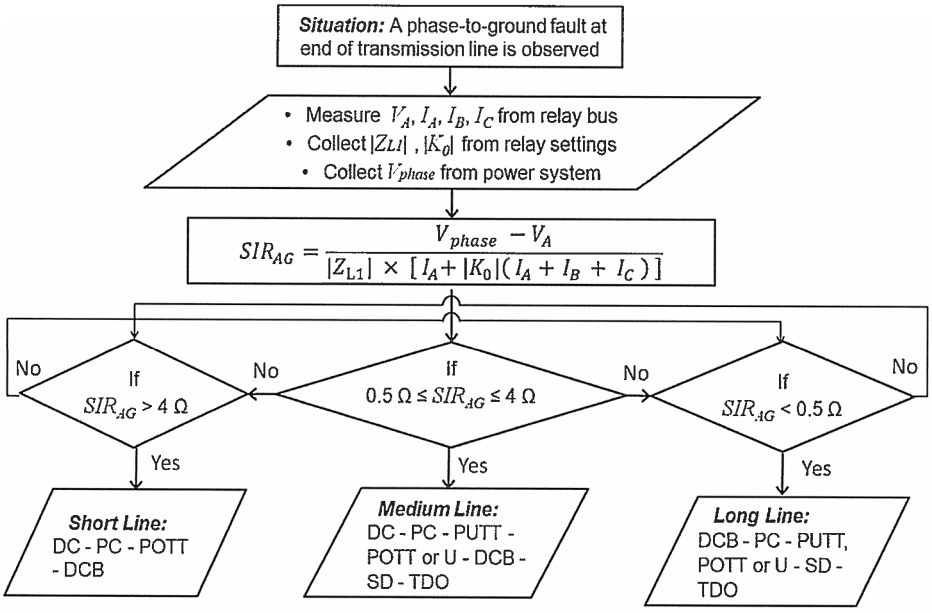

Fig. 3. Flowchart of recommended protection schemes for short, medium and long transmission lines.

relays. The tests were performed for a phase-to-ground fault, that is the most common fault in power transmission lines [19]. The two fault locations cases were set at 10 and 100% of the line length, as measured from the relay location. In distance relays, Zone 1 and 2 are usually set at 80 and 120% of the impedance of the transmission line length, respectively [20]. Because Zone 2 represents the limit to detect the faults inside of the transmission line, only Zone 2 was plotted with the phase-to-ground apparent impedance paths (represented by circles in the R–X diagram, for instance as shown in Figs. 7–10). Following the onset of a phase-to-ground fault, the model shows the path of the apparent impedance progressing towards the interior of the reference circle in the R–X diagram. In this study, the mho relay model needed to operate properly while the GIC NBDs are inserted, and the SIRs for both 230 and 345 kV lines during the phase-to-ground fault were compared with and without GIC NBDs.

3. Methodology

3.1. The power system

The power system was simulated by the network shown in Fig. 1. This network includes one utility source, two three-phase delta-wye transformers, one transmission line (considered, separately for both the 230 and 345 kV cases) and a load. The network configuration was based

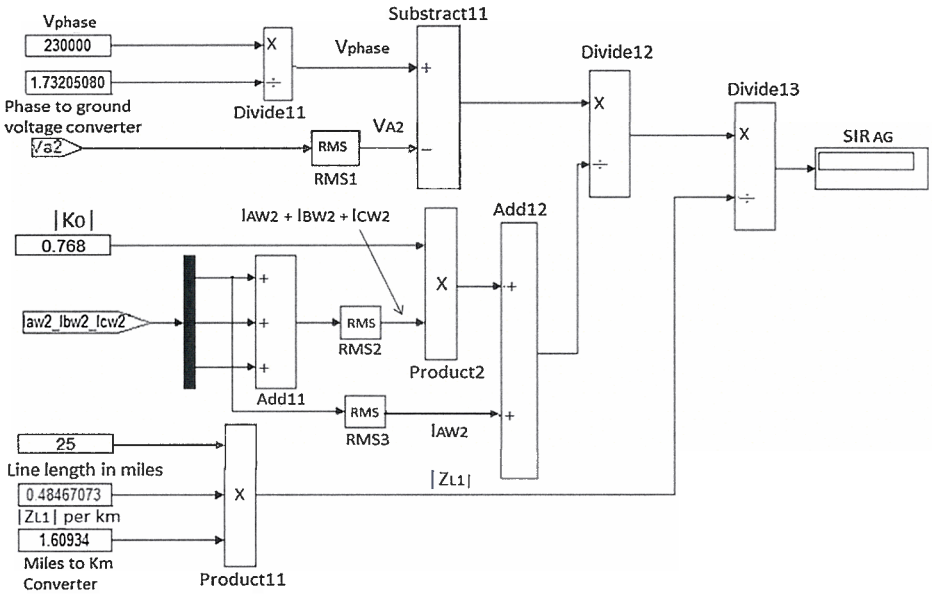

Fig. 4. RT-LAB Block to compute the SIR for the phase-to-ground fault (e.g. for the 230 kV transmission line).

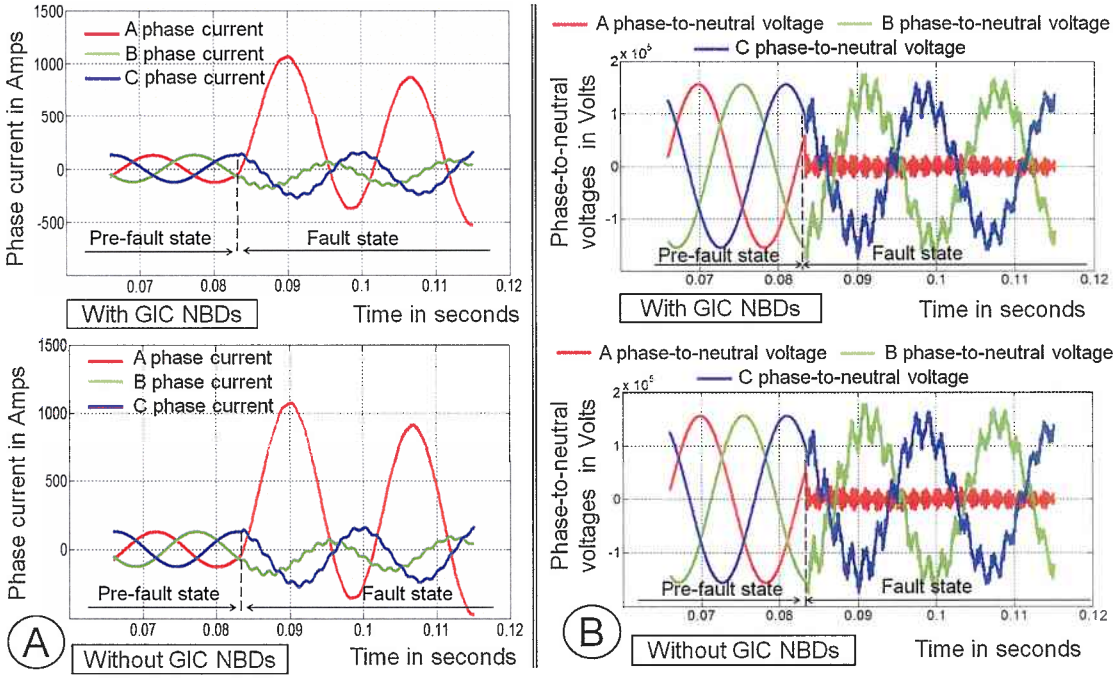

Fig. 5. Currents (A) and phase-to-neutral voltages (B) for the ZAG_10%_25_230_2650 test.

on a radial power system. The transmission lines were simulated with a MATLAB® three-phase PI section line block. This model consisted of one set of resistor-inductor series elements connected between input and output terminals, and two sets of shunt capacitances lumped at both ends of the line. The transmission line extremes were connected to one three-phase transformer. The delta- wye transformers were simulated with a MATLAB® three-phase two-winding transformer block. This model implemented a three-phase transformer by using single-phase transformers. The GIC NBDs were connected to the wye neutral winding of three-phase transformers. A switch near the load allowed to test the effect of inserting the GIC NBDs (with three options: 2650/265/26.5 μF) in place of the direct grounding option. This allowed to consider the different cases comparing the line apparent impedance changes resulting from a phase-to-ground fault.

In this study, the RT-LAB® and MATLAB® software tools were used to simulate a transmission line, using an OP4510 real-time simulator. The transmission line was simulated with "π line model" block, the values positive and zero-sequence impedances per unit length, for both cases of 230 and 345 kV that were considered, are shown in Table 1.

3.2. Phase-to-ground fault apparent impedance

The distance protection relays operate based on the measure of the apparent impedances to detect faults in transmission lines. Considering phase A, for instance, the phase-to-ground fault apparent impedance Z_{ag} is computed based on the instantaneous voltages and currents as [21]:

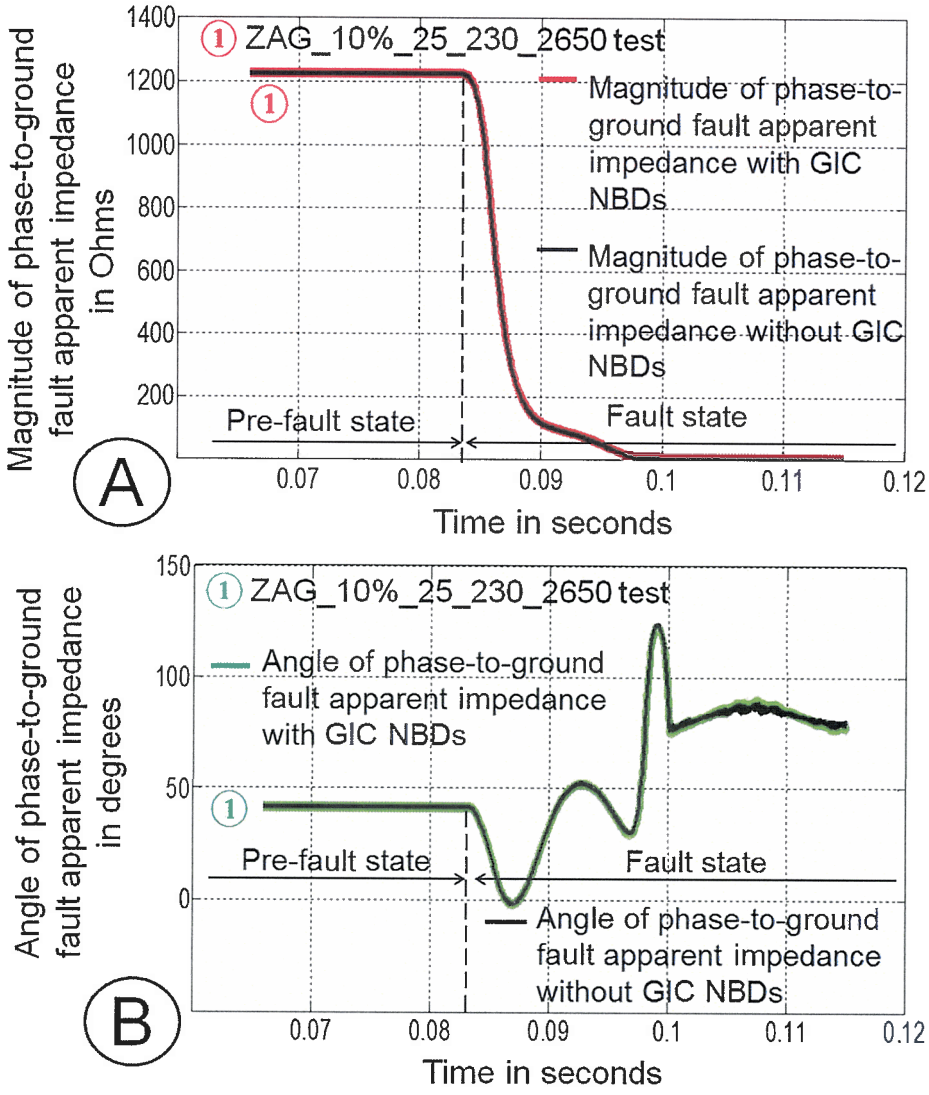

Fig. 6. Phase-to-ground fault apparent impedance magnitude (A) angle (B) at the ZAG_10%_25_230_2650 test.

$$Z_{ag} = \frac{V_a}{I_a + K_0\,(3I_0)} = \frac{V_a}{I_a + K_0(I_a + I_b + I_c)} \tag{1}$$

where Z_{ag} is the A phase-to-ground fault apparent impedance, V_a is the A phase-to-neutral voltage, I_a is the A phase current (and similarly for I_b and I_c), $I_0 = (I_a + I_b + I_c)/3$ is the zero-sequence current, and K_0 is the zero-sequence current compensation factor given by [21]

$$K_0 = \frac{Z_{L0} - Z_{L1}}{3Z_{L1}} \tag{2}$$

In (2) Z_{L0} and Z_{L1} are, respectively, the zero- and positive-sequence impedances of the transmission line, expressed (in standard complex notation with i as the imaginary unit) as

$$Z_{L1} = (rl_1 \times l) + i(xl_1 \times l) \tag{3}$$

$$Z_{L0} = (rl_0 \times l) + i(xl_0 \times l) \tag{4}$$

where l is the length of the transmission line, rl_1 and rl_0 are the positive- and zero-sequence per unit length (p.u.l.), respectively, xl_1 and xl_0 are the positive and zero-sequence series reactance (p.u.l.), respectively.

K_0 can be then computed from (2), (3) and (4), and with rl_1, xl_1, rl_0 and xl_0 as defined Table 1. Examples for the K_0 values computed for 25, 50 and 100 miles transmission line lengths, and at 230 and 345 kV are shown in Table 2.

The phase-to-ground fault apparent impedance was computed by implementing the definition (1) in RT-LAB®, and using the instantaneous values for the phase-to-neutral voltages and phase currents simulated in the model. Fig. 2 shows the actual RT-LAB® implementation scheme, that can also be used without modifications for a hardware-in-the-loop, real-time simulation, by simply replacing the simulated relay block in Fig. 1 with an actual relay unit connected to the OP4510.

The RT-LAB Block to compute the phase-to-ground fault apparent impedance is shown in Fig. 2. The phase-to-ground fault apparent impedance was computed as in (1) as in the RT-LAB block implementation of Fig. 2. This RT-LAB Block collected the A phase-to-neutral voltage at Bus 1 (Fig. 1), and A, B and C phase currents at Breaker (Fig. 1). Before running the simulation tests, this RT-LAB Block was set with the zero sequence compensation factors K_0 for each transmission line, based on Table 2. The magnitude and angle of the phase-to-ground fault apparent impedance were plotted while the simulation was running and were recorded to compare the results with and without the blocking capacitors (2650 μF, 265 μF and 26.5 μF) inserted on the neutral transformers.

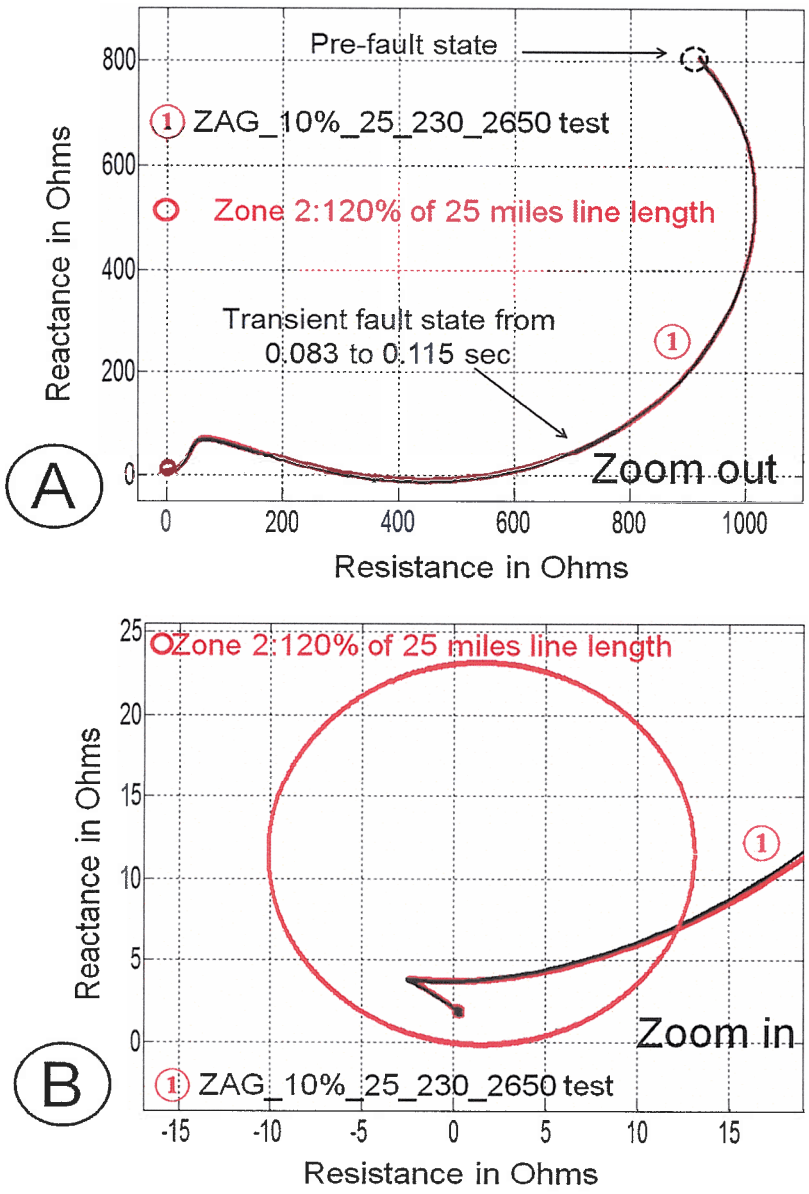

Fig. 7. Zoom out (A) and zoom in (B) at the ZAG_10%_25_230_2650 test.

3.3. Source-to-line impedance ratio

In distance protection relays, the transmission line length is defined by the source-to-line impedance ratio (SIR) [22,23] that is used to determine the protection schemes. The SIR is the preferred method to classify the electrical length of transmission lines to select the proper distance protection relay settings.

The SIR can be computed with a short circuit condition at the line termination [23], as it refers to a realistic condition to which a distance relay may be exposed. By referring to phase A (analogous definitions will apply to B and C phases), the magnitude of the source impedance for a phase to ground fault ($Z_{S,AG}$) was calculated by the primary voltage drop from the source to the relay location (V_{SRA}), divided by the primary current (I_{RA}) at the relay for a fault at remote bus [23]:

$$|Z_{S,AG}| = \frac{V_{SRA}}{I_{RA}} \tag{5}$$

In (5) V_{SRA} is computed as the difference between the nominal phase-to-ground voltage V_{phase} and the actual measured phase-to-neutral voltage at the relay location V_A:

$$V_{SRA} = V_{phase} - V_A \tag{6}$$

I_{RA} is the relay current computed for the phase-to-ground fault apparent impedance, as in the denominator in (1), but represented by the magnitudes of primary values. The relay current for phase-to-ground fault case is expressed by

$$I_{RA} = I_A + |K_0|\ (I_A + I_B + I_C) \tag{7}$$

By applying (6) and (7) in (5), the magnitude of the source impedance for the phase-to-ground fault loop $Z_{S,AG}$ can be written as

$$|Z_{S,AG}| = \frac{V_{phase} - V_A}{I_A + |K_0|\ (I_A + I_B + I_C)} \tag{8}$$

The SIR for the phase-to-ground fault case, SIR_{AG}, is then the ratio of the magnitude of source impedance $Z_{S,AG}$ and the magnitude of the positive sequence impedance of the transmission line, and it is expressed according to [23]:

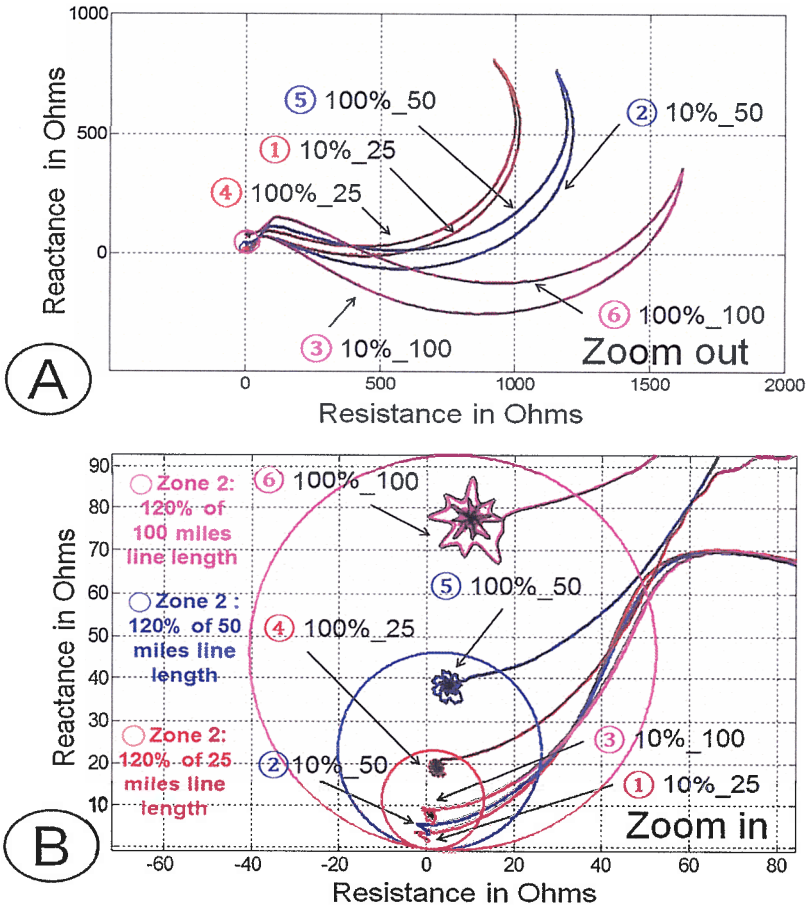

Fig. 8. Phase-to-ground fault apparent impedances for 230 kV (A–B) transmission lines of 25, 50, and 100 miles length without and with 2650 μF GIC NBDs.

$$SIR_{AG} = \frac{|Z_{S.AG}|}{|Z_{L1}|} \tag{9}$$

Therefore, by replacing (8) in (9), it is found:

$$SIR_{AG} = \frac{V_{phase} - V_A}{|Z_{L1}|\,[\,I_A + |K_0|\,(I_A + I_B + I_C)\,]} \tag{10}$$

A short line may pose a challenge in terms of protection settings because it makes it difficult for the relay to differentiate between a fault inside (in-zone) and outside (out-of-zone) at a given distance protection zone [22]. Therefore, distance protection guidelines provide the setups for short lines that are defined to detect the line in-zone faults [24–26]. The setups for medium and long lines are defined to detect the line in-zone and out-of-zone faults. The recommended protection schemes for distance relays depend on whether transmission lines are classified as short, medium or long [22,24]. Fig. 3 shows a flowchart of recommended protection schemes for short, medium and long transmission lines.

In the flowchart of Fig. 3, the SIR for the phase-to-ground fault was computed as in (10) as in the RT-LAB block implementation of Fig. 4. In this case the magnitudes of primary values of the phase currents and the phase-to-neutral voltages (from the Breaker and Bus 1 of Fig. 1) provided the required magnitude values in (10). The RMS blocks (Fig. 4) computed the true root mean square value of the input signal over a running average window of one cycle.

4. Results

The phase-to-ground fault apparent impedances and the source impedance ratios for the phase-to-ground fault loop were computed to assess the impact on distance protection operations, for 230 and 345 kV transmission lines. The simulations were performed with and without the blocking capacitors (2650 μF, 265 μF and 26.5 μF) inserted on the neutral of both transformers on each side of the transmission line. The test results were recorded by an "OpWriteFile" block, and analyzed in MATLAB®. The test runs (including a pre-fault interval) considered a total simulated time of 0.25 s, with the fault occurring at 0.083 s (5/60 cycles). All tests were run with an OP4510 real-time simulator set with a 50 μs time step. Figs. 5 and 6 show the results of a test with the phase-to-ground fault apparent impedance (ZAG) located at 10 % of the 25-mile long line, at 230 kV, and with the 2650 μF GIC NBD (as summarized by the label "ZAG_10%_25_230_2650". In this case, the results were plotted from 0.066 to 0.115 s to observe in detail the transients shortly after the phase-to-ground fault at 0.083 s. The A, B and C phase currents and phase-to-neutral voltages are shown in Fig. 5A and B, respectively. The phase currents and voltages waveforms were similar with and without GIC NBDs.

The magnitude (red) and angle (green) for the phase-to-ground fault apparent impedance in the radial power system with GIC NBDs (2650 μF) are shown in Fig. 6A and B, respectively. The magnitude and angle (black) for the phase-to-ground fault apparent impedance in the radial power system without GIC NBDs are also shown. In Fig. 6, the magnitude and angle showed virtually identical patterns for the phase-to-ground fault apparent impedances with and without GIC NBDs.

In Fig. 7, the results for the ZAG_10%_25_230_2650 test are plotted. The paths for the phase-to-ground fault apparent impedances with and without GIC NBDs are in red and black, respectively. In Fig. 7A (zoom-out), the whole path of the phase-to-ground fault apparent impedance is shown. A detail of the path of the phase-to-ground fault apparent

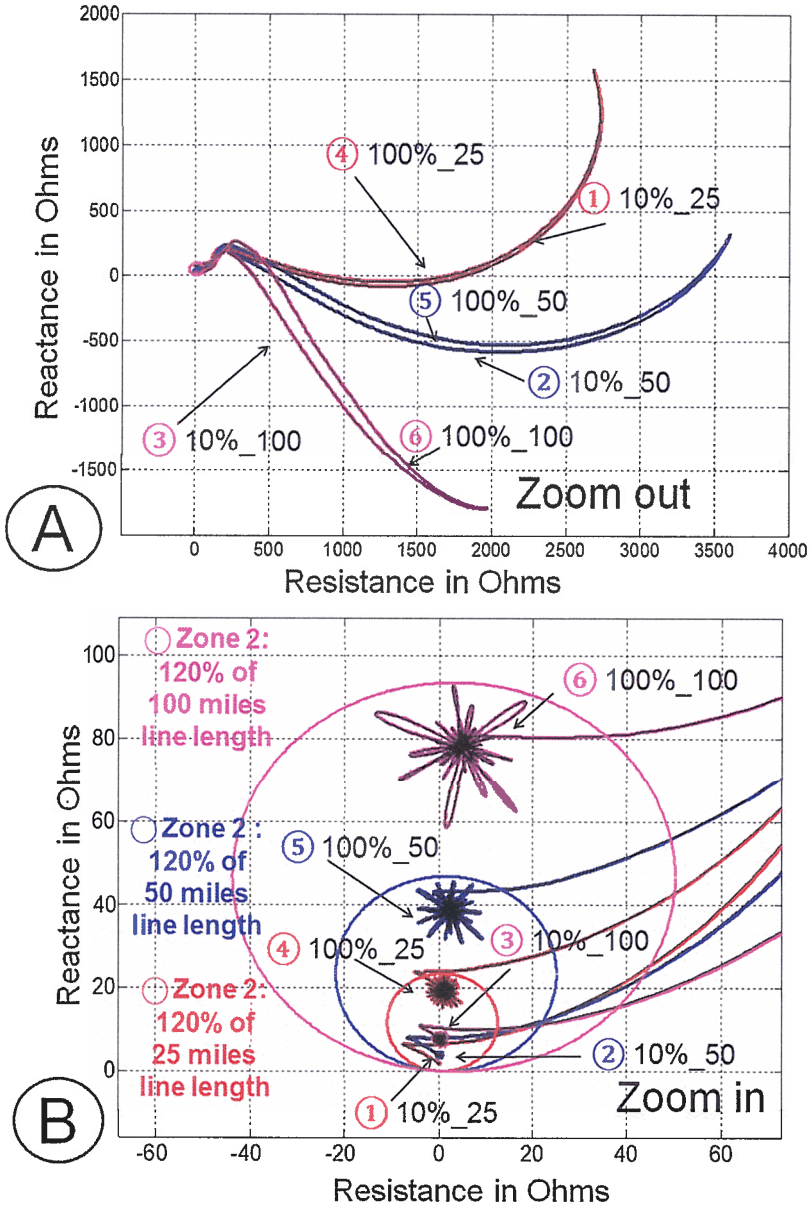

Fig. 9. Phase-to-ground fault apparent impedances for 345 kV (A–B) transmission lines of 25, 50, and 100 miles length without and with 2650 μF GIC NBDs.

impedance reaching the internal area of the R–X circle, when the distance relay operates, is shown in Fig. 7B (zoom-in). In Fig. 7A and B, the red and black paths showed virtually identical patterns, indicating that the same behavior for the measured phase-to-ground fault apparent impedances occurs with and without GIC NBDs.

The tests for the 230 kV transmission lines are reported in Fig. 8 A and B, that illustrate the phase-to-ground fault apparent impedances paths at 10 and 100 % of line lengths, for the 25, 50 and 100-mile long transmission lines, and using a 2650 μF GIC NBD. In the R–X diagrams, are the distance protection zones of 120 % (Zone 2) are shown as red, blue and pink circles for the 25, 50 and 100-mile length, respectively. These paths are the measured phase-to-ground fault apparent impedances during the pre-fault (from 0 to 0.083 s.) and fault (from 0.083 to 0.25 s.) states. The black curves are the paths of the phase-to-ground fault apparent impedances for the transmission lines without GIC NBDs (referenced values). The phase-to-ground fault apparent impedances for the 25, 50 and 100-mile long transmission lines at 230 kV showed similar behaviors with and without 2650 μF GIC NBDs.

Similarly, Fig. 9 A and B refer to the 345 kV transmission line, showing again the phase-to-ground fault apparent impedances at 10 and 100% of line lengths for the 25, 50 and 100-mile long transmission lines, respectively, with 2650 μF GIC NBDs. The circles and the apparent impedance paths in the R–X diagrams are the same as described in Fig. 8. As for the 230 kV case, the phase-to-ground fault apparent impedances for the 25, 50 and 100-mile long transmission lines at 345 kV showed similar behaviors with and without 2650 μF GIC NBDs.

In this study, non-typical values of GIC NBD capacitance (26.5 and 265 μF) were also tested and compared with conventional grounding, for 50-mile long at 230 and 345 kV transmission lines (Fig. 10). In the R–X diagrams, the blue circle represents 120% of the transmission line length (Zone 2).

These results indicated that performance was better with the larger capacitors (2650 and 265 μF) than with the smaller 26.5 μF ones. In fact, the 26.5 μF case shows a pronounced difference compared with the conventional grounding, as can be seen by observing the different paths for the phase-to-ground fault apparent impedances. However, mho

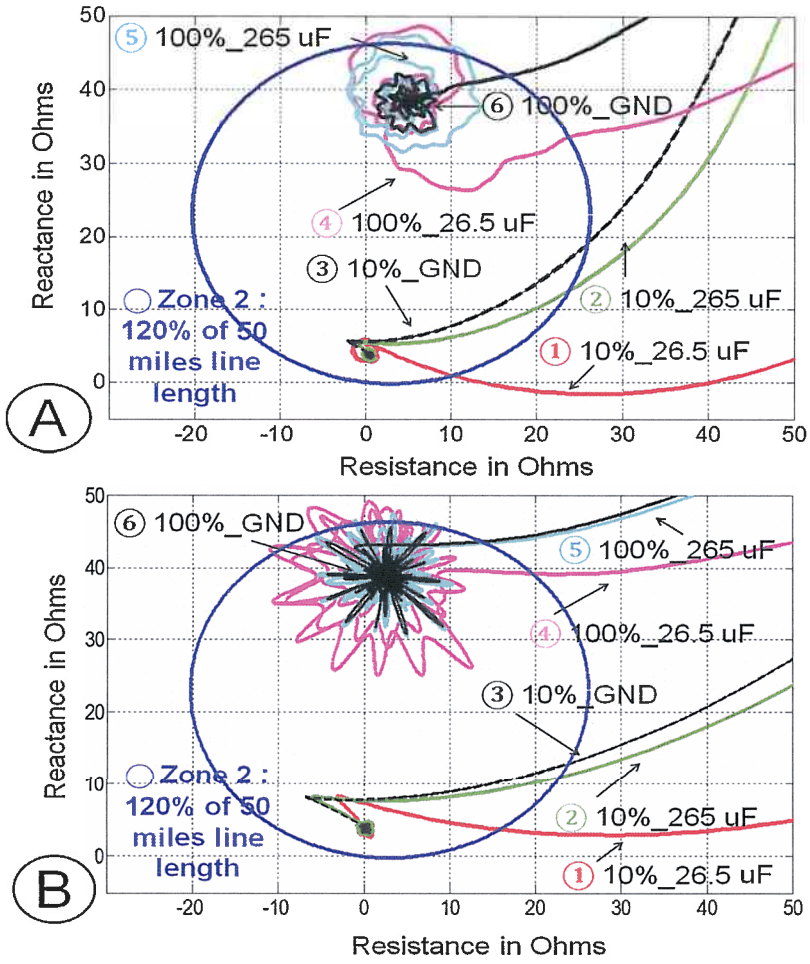

Fig. 10. Phase-to-ground fault apparent impedances for 230 kV (A) and 345 kV (B) transmission lines of 50 miles length without and with 26.5 and 265 μF GIC NBDs.

Table 3
Phase-to-ground fault apparent impedance for 230 and 345 kV lines with and without GIC NBDs.

Line Voltage Level		230 kV Line					345 kV Line				
Line Length in km [miles]		160.94 [100]	80.46 [50]			40.23 [25]	160.94 [100]	80.46 [50]			40.23 [25]
GIC NBDs [μF]		2650	2650	265	26.5	2650	2650	2650	265	26.5	2650
Fault at 100% of line length	Agreement between phase-to-ground fault apparent impedance paths with and without GIC NBDs at transient fault state.	Good Fig. 8 (B) Curve ⑥	Good Fig. 8 (B) Curve ⑤	Fair Fig. 10 (A) Curve ⑤	Poor Fig. 10 (A) Curve ④	Good Fig. 8 (B) Curve ④	Good Fig. 9 (B) Curve ⑥	Good Fig. 9 (B) Curve ⑤	Fair Fig. 10 (B) Curve ⑤	Poor Fig. 10 (B) Curve ④	Good Fig. 9 (B) Curve ④
	Phase-to-ground fault apparent impedance inside the circle in the R-X diagram at permanent fault state.	Yes Fig. 8 (B) Curve ⑥	Yes Fig. 8 (B) Curve ⑤	Yes Fig. 10 (A) Curve ⑤	Yes Fig. 10 (A) Curve ④	Yes Fig. 8 (B) Curve ④	Yes Fig. 9 (B) Curve ⑥	Yes Fig. 9 (B) Curve ⑤	Yes Fig. 10 (B) Curve ⑤	Yes Fig. 10 (B) Curve ④	Yes Fig. 9 (B) Curve ④
Fault at 10% of line length	Agreement between phase-to-ground fault apparent impedance paths with and without GIC NBDs at transient fault state.	Good Fig. 8 (B) Curve ③	Good Fig. 8 (B) Curve ②	Fair Fig. 10 (A) Curve ②	Poor Fig. 10 (A) Curve ①	Good Fig. 8 (B) Curve ①	Good Fig. 9 (B) Curve ③	Good Fig. 9 (B) Curve ②	Fair Fig. 10 (B) Curve ②	Poor Fig. 10 (B) Curve ①	Good Fig. 9 (B) Curve ①
	Phase-to-ground fault apparent impedance inside the circle in the R-X diagram at permanent fault state.	Yes Fig. 8 (B) Curve ③	Yes Fig. 8 (B) Curve ②	Yes Fig. 10 (A) Curve ②	Yes Fig. 10 (A) Curve ①	Yes Fig. 8 (B) Curve ①	Yes Fig. 9 (B) Curve ③	Yes Fig. 9 (B) Curve ②	Yes Fig. 10 (B) Curve ②	Yes Fig. 10 (B) Curve ①	Yes Fig. 9 (B) Curve ①

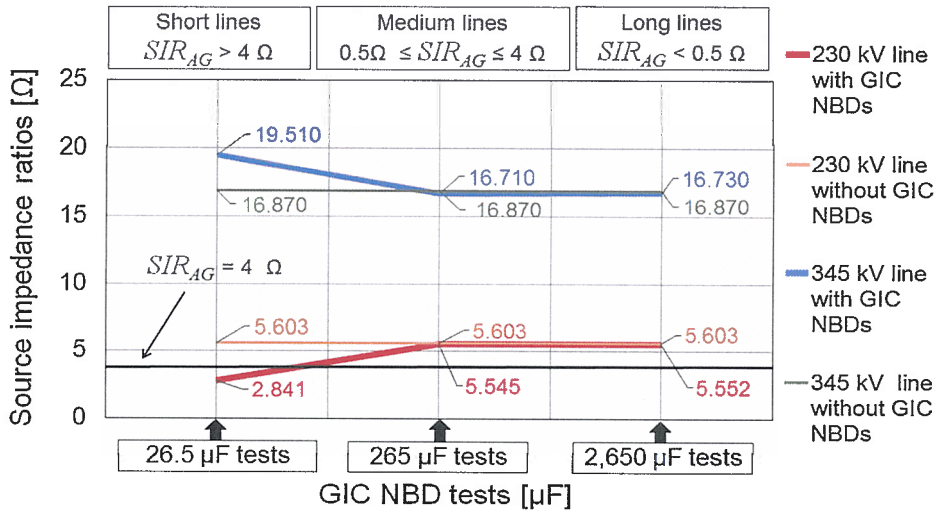

Fig. 11. Source impedance ratio for phase-to-ground fault at 230 and 345 kV transmission lines of 50 miles length without and with 26.5, 265 and 2650 μF GIC NBDs.

distance relays are expected to trip anyway, because the phase-to-ground apparent impedance path end inside the blue circle (that indicates the operation zone for the distance relay). It should be noted that the 26.5 μF case, however, is far from typical values required for actual installations, and represents a limit scenario considered as a verification that the model can capture the proper dynamics.

In Fig. 10, the oscillation of the phase-to-ground fault apparent impedance for faults located at 100% of the transmission line length were due to the capacitance added along the transmission line. This was because currents and voltages at fault states were superimposed on the fundamental frequency component due to the capacitance of the transmission line. This harmonic component can cause the oscillation of the distance measurements [27], and it can be filtered from the phase-to-ground fault apparent impedance for faults located at 100% of the transmission line length by implementing typical microprocessor relay filtering [28,29].

Figs. 8–10 show how the paths of the phase-to-ground fault apparent impedances, with GIC NBDs with different capacitance values, compare with the conventional case of conductor grounding. As are summarized in Table 3, these comparisons indicate that the paths for 2650, 265 and 26.5 μF capacitors show, respectively, a good, fair, and poor matching, with the path of the direct grounding case. However, all the impedance path terminations, corresponding to the permanent fault state, are located inside the circle in the R–X diagram, thus demonstrating that the mho distance relays are expected to provide the required protection in all cases.

The SIRs for the phase-to-ground fault (phase A) were computed according to Eq. (10), and the results for the cases of 50-mile length, at 230 and 345 kV and with and without 26.5, 265 and 2650 μF GIC NBDs are shown in Fig. 11. The SIRs curves with direct grounding, 265 and 2650 μF show minor differences. However, the SIR with a 26.5 μF GIC NBD had appreciable differences compared with the direct grounding, showing a 49% variation for the 230 kV case, and 16% for the 345 kV. In the 230 kV case, the SIRs with the 26.5 μF capacitor (red curve) became smaller than 4 Ω (the SIR defining threshold to distinguish a shorth from a medium transmission line). Thus, the same 50-mile line was considered a medium line length with the 26.5 μF GIC NBD, while it was a short line length with larger capacitors or direct grounding. Therefore, protection schemes (Fig. 3) should be chosen accordingly. Again, it should be recalled that the 26.5 μF case does not represent a choice that would be considered in actual GIC protection installations, and it is here discussed to provide a reference for the lower limit of the capacitance value range.

The results of this study were validated in a previous publication [8] that investigated the operation of distance relays at IEEE-39 bus system with GIC NBDs, implemented by a real-time simulator with hardware in-the-loop. The previous study [8] showed that distance relays were not affected by the insertion of GIC NBDs. On the other hand, a report [30] that discussed the early development and testing of GIC NBDs did not report fault events. Another publication [31] addressed that transmission line-to-ground faults were not reported during Geomagnetic Disturbances (GMDs) that might have triggered the updated engineering system model to test fault protection functions [31]. Therefore, there are no protection fault data on the performance of the updated engineering system model during potentially damaging because of GMDs.

5. Conclusions

This study, conducted on a real-time power system simulator, provided a satisfactory evaluation of the impact of GIC neutral blocking devices on mho distance relay operations for different values of transformer neutral capacitors, and for different transmission line voltages. In the simulations, phase-to-ground fault scenarios at different line locations were considered, and the apparent impedance evolution during the transient was measured at the relay location. The present model, by design, can also be used without any modifications for a hardware in-the-loop distance relay implementation with the OP4510 simulator.

The model was used to study the impact of insertion of GIC NBDs on distance protection relay operations. The most realistic case uses 2650 μF capacitors, and resulted in no negative impact on the ability to operate the distance relay properly, in response to a phase-to-ground fault. The tests were performed for 230 and 345 kV transmission lines of 25, 50 and 100 miles in length. The R–X diagram paths were compared for the phase-to-ground fault apparent impedances, with and without GIC NBDs. Compared to direct grounding, no meaningful differences in the apparent impedance path occurred with the 2650 μF GIC NBD insertion (Figs. 8 and 9). In addition, 265 and 26.5 μF GIC NBD tests were also performed, now only for the 50-mile transmission line length (the most sensitive case) and at both 230 and 345 kV. As summarized in Table 3, the comparison of phase-to-ground fault apparent impedance paths with and without GIC NBDs at transient fault state showed, good, fair, and poor path match, respectively for 2650, 265, and 26.5 μF capacitors. However, for all the three values of capacitance considered, the termination of impedance path, corresponding to the permanent fault state, was always inside the circle in the R–X diagram, demonstrating that mho distance relays are expected to operate properly in any of the cases considered.

The SIRs for a phase-to-ground fault, of 50 miles length at 230 and 345 kV were also computed for the same three different capacitor values (Fig. 11). The 26.5 μF GIC NBD showed a pronounced difference in the computed SIRs compared with the other capacitance values. The insertion of this relatively small capacitance (for the 50-mile case under consideration) resulted in a change in the qualification of the line length in terms of SIR from "small" to "medium", thus requiring a different relay setting. This case, however, is far from typical design values for actual installations, and represents a worst-case, limit scenario that was considered to verify that the model can capture the expected dynamics.

This study outlined a general methodology that can be applied in a wide variety of cases to analyze the feasibility of GIC NBDs protections in complex grid layouts. With a continuous monitoring of GIC NBDs early installations, additional data on the dynamic response during fault on distance protection relays can be made available. This data can then be used to benchmark the results obtained with the proposed methodology, thus providing the necessary confidence for a larger-scale installation of GIC-NBDs. In the future, the collection of protection fault data on the updated electrical engineering systems during potentially damaging because of GMDs will be crucial to study the performance of distance relays.

Finally, as an avenue for further developments, the utilization of adaptive distance protection schemes can be considered to enhance the feasibility of GIC NBDs installations. For instance, that may result beneficial in cases where the blocking capacitance leads to a change in the SIR qualification of the line length, thus requiring switching to different relay settings. The possible occurrence of these conditions, aside from the use of exceedingly small capacitances (as was shown in this work), could be perhaps found in a more complex grid topology than the basic case here considered.

Conflict of interest

None declared.

References

[1] L. Bolduc, et al., Development of a DC current-blocking device for transformer neutrals, IEEE Trans. Power Deliv. (January) (2005) 163–168.
[2] F.R. Faxvog, et al., HV power transformer neutral blocking device (NBD) operating experience in Wisconsin, MYPSICON, November, 2017, pp. 1–15.
[3] R. Girgis, K. Vedante, Effects of GIC on power transformers and power systems, IEEE PES T&D Conference, Orlando, FL USA. May, 2012, pp. 1–8.
[4] J. Kappenman, Low-Frequency Protection Concepts for the Electric Power Grid: Geomagnetically Induced Current (GIC) and E3 HEMP Mitigation, Meta-R-322 Report, Metatech Corporation and Oak Ridge National Laboratory, 2010, pp. 1–94 January.
[5] H. Zhu, T.J. Overbye, Blocking device placement for mitigating the effects of geomagnetically induced currents, IEEE Trans. Power Syst. (July) (2015) 1–9.
[6] S.K. Vijapurapu, Contingency Analysis of Power Systems in Presence of Geomagnetically Induced Currents, Master of Science Thesis, Department of Electrical and Computer Engineering, College of Engineering, University of Kentucky, 2013, pp. 1–117.
[7] M. Kamel, et al., Effects of GIC neutral blocking devices (NBDs) on transmission lines protection performance and potential for resonance, CIGRE US National Committee, Grid of the Future Symposium (2015) 1–14.
[8] H. Saeed, Effects of GIC Neutral Blocking Devices (NBDs) on Transmission Lines Protection Performance and Potential for Resonance, Master of Science Thesis, The University of Tennessee at Chattanooga, 2015, pp. 1–57 December.
[9] R. Girgis, K. Vedante, K. Gramm, Effects of geomagnetically induced currents on power transformers and power systems, CIGRE (2012) 1–8. A2-304.
[10] M. Kazerooni, Hao Zhu, T.J. Overbye, Mitigation of geomagnetically induced currents using corrective line switching, IEEE Trans. Power Syst. (May) (2018) 2563–2571.
[11] M. Lu, et al., Optimal transmission line switching under geomagnetic disturbances, IEEE Trans. Power Syst. (May) (2018) 2539–2550.
[12] A. Rezaei-Zare, A.H. Etemadi, Optimal placement of GIC blocking devices considering equipment thermal limits and power system operation constraints, IEEE Trans. Power Deliv. (February) (2018) 200–208.
[13] P. Yang, et al., Optimal placement of grounding small resistance in neutral point for restraining voltage fluctuation in power grid caused by geomagnetic storm, IET Trans. Gener. Transm. Distrib. (April) (2019) 1456–1465.
[14] F.R. Faxvog et al., Power Grid Protection against Geomagnetic Disturbances (GMD), 2013 IEEE Electrical Power & Energy Conference, pp. 1–13.
[15] J. Roberts, A. Guzman, E.O. Schweitzer III, Z = V/I does not make a distance relay, 48th Annual Georgia Tech Protective Relaying Conference Atlanta, Georgia, May 4-6, 1994, pp. 1–20.
[16] D.D. Fentie, Understanding the Dynamic Mho Distance Characteristic, 2016 Texas A &M Conference for Protective Relay Engineers, pp. 1–15.
[17] D. Shi et al., Transmission line parameter identification using PMU measurements, pp. 1–17.
[18] S.M. Westervelt, Transmission Line Positive Sequence Parameter Determination Using Synchronized Phasor Measurements, Master of Science Thesis, Department of Engineering and the faculty of the Graduate School, Wichita State University, 2015, pp. 1–136 May.
[19] L. Wang, The fault causes of overhead lines in distribution network, MATEC Web of Conferences, APOP, 2016, pp. 1–5.
[20] Network Protection & Automation Guide, Distance Protection, Chapter 11, pp. 171–191.
[21] F. Calero, Distance Elements: Linking Theory with Testing, 2009 Texas A&M Conference for Protective Relay Engineers, pp. 1–20.
[22] IEEE Standard C37.113-2015, IEEE Guide for Protective Relay Applications to Transmission Lines, June (2016).
[23] M.J. Thompson, A. Somani, A Tutorial on Calculating Source Impedance Ratios for Determining Line Length, Schweitzer Engineering Laboratories, Inc, ProRelay, 2015, pp. 833–841.
[24] Distance Protection Schemes & Relay Settings applied to Multiterminal Lines, Electrical Safety, April 2018, Available: http://engineering.electrical-equipment.org/safety/distance-protection-schemes-relay-settings-applied-multiterminal-lines.html.
[25] S. Ganesan, E. Price, REL 512 Setting Example for Short Lines, AN-60L-00ABB Application Note, Substation Automation and Protection Division, March, Available: (2003), pp. 1–18 http://www.abb.com/abblibrary/downloadcenter/?View=Result.
[26] G.E. Alexander, J.G. Andrichak, and W.Z. Tyska, Relaying Short Lines, General Electric, GE Power Management, pp. 1–13. Available: http://store.gedigitalenergy.com/faq/listing.asp.
[27] T. Kase, Y. Kurosawa, H. Amo, Charging current compensation for distance protection, IEEE Trans. Power Deliv. 23 (January (1)) (2008) 124–131.
[28] G.E. Alexander, J.G. Andrichak, Ground distance relaying: problems and principles, GER-3793, General Electric Company, Nineteenth Annual Western Protective Relay Conference Spokane, Washington, October 20, 1991, pp. 1–36.
[29] E. Price, T. Einarsson. Complementary approach for reliable high speed transmission line protection, 61st Annual Conference for Protective Relay Engineer, College Station, TX, USA, 1–3 April, 2008, pp. 1–10.
[30] P.R. Barnes et al., Experience with Geomagnetic Disturbances, Oak Ridge National Laboratory, ORNL-6665 Report, pp. 1–94. Available: https://www.osti.gov/biblio/10108452.
[31] Critical Infrastructure Protection, Protecting the Electric Grid from Geomagnetic Disturbances, GAO United States Government Accountability Office, GAO-19-98 Report, December 2018, pp. 1–55. Available: https://www.gao.gov/products/GAO-19-98.

Emilio C. Piesciorovsky graduated as an Electrical Engineer from the National Technological University, Argentina (1995). He received his master's degree in Marketing from La Plata National University, Argentina (2001). He worked as Sales Manager for Pirelli Power Cables and Systems, and S.D.M.O. Industries. He worked as a Senior Engineer and Protection & Control Engineer III for A.B.B. and Casco Systems, respectively. He completed his M.S. (2009) and Ph.D. (2015) degrees in Electrical Engineering from Kansas State University, USA. Then, he worked as a Postdoc Research Associate at the Center for Energy Systems Research, Tennessee Technological University and Oak Ridge National Laboratory. Currently, he is a Professional Technical Staff III in the Power System Protection area at Oak Ridge National Laboratory; piesciorovec@ornl.gov.

Alfonso G. Tarditi completed his academic education at the University of Genoa, in Genoa, Italy (B.S. and M.S. in Electronics Engineering, 1985, Doctorate in Electrical Engineering, 1990). In the next two years he was awarded a N.A.T.O. post-doctoral fellowship at UC Berkeley. Since that time he was involved in fusion research, that continued first after joining the Lawrence Livermore National Laboratory, and then with Science Application International Corporation. He then held positions as Sr. Scientist with contractors at the NASA Johnson Space Center (Houston, TX), leading R&D in electromagnetic compatibility, and in space propulsion and power systems. During that time, he also taught Plasma Physics and Electrodynamics at the University of Houston. After serving as a project manager at the Electric Power Research Institute, and as Chief Scientist at NPL Associates Inc. (Urbana, IL), focused on plasma and nuclear technologies, he joined the Senior R&D staff at the Oak Ridge National Laboratory; tarditiag@ornl.gov.